Polymer Chemistry

ROYAL SOCIETY OF CHEMISTRY

PAPER

View Article Online
View Journal | View Issue

Cite this: *Polym. Chem.*, 2026, **17**, 2437

Thioamides on radical-chain growth monomers: post-polymerization transformation for tailored functional polymers

Selin Kinali-Demirci, Serkan Demirci * and Brett VanVeller *

Thioamides cannot be easily incorporated into radical chain-growth polymers because they react rapidly with propagating radicals, preventing vinyl monomers bearing thioamides from undergoing efficient radical polymerization. As a result, thioamide-containing polymers are largely restricted to step-growth strategies or inefficient post-polymerization thionation methods. Here, we address this limitation using thioimidates as radical-compatible precursors to thioamides. Thioimidate-functionalized monomers undergo conventional free-radical copolymerization to give linear and cross-linked copolymers, demonstrating that thioimidate groups are compatible with radical chain-growth conditions. Subsequent treatment with NaHS converts thioimidates to thioamides within minutes at room temperature, producing only gaseous by-products and avoiding the heterogeneous side reactions associated with traditional sulfurizing reagents. The resulting thioamide-functional copolymers are characterized, and their ability to bind gold from aqueous solution is demonstrated as a proof of concept rather than an optimized recovery process. Together, these results establish a general strategy for accessing thioamide-functional chain-growth copolymers and highlight thioimidates as a versatile platform for post-polymerization conversion to thioamides.

Received 7th April 2026,
Accepted 18th May 2026

DOI: 10.1039/d6py00344c

rsc.li/polymers

Introduction

Thioamides are single-atom isosteres of the amide bond that have served as design elements across peptide, medicinal, and materials chemistry.[1–3] Relative to the amide, thioamides display altered hydrogen-bonding behavior,[4–7] greater lipophilicity,[8,9] resistance to proteolysis,[10,11] along with other distinct physicochemical properties.[12,13]

Thioamide-containing polymers represent a growing class of functional materials that combine the unique properties of thioamides with the processability and versatility of polymeric systems.[14–18] A key advantage of thioamide-containing polymers is their strong metal-ion coordination and exceptional affinity for precious metals including mercury, platinum, palladium, and gold from aqueous solutions.[19–22] This selective metal-binding behavior has found applications in metal recovery, environmental remediation, and sensing technologies.[22–24]

Despite this promise, thioamides remain largely inaccessible in chain-growth polymers. Vinyl monomers bearing thioamides in the side chain cannot undergo radical polymerization because radical addition to the thioamide is kinetically favored over propagation,[25] although bulky thioamide monomers with carefully designed structures have recently been shown to be amenable to direct radical copolymerization.[26] Consequently, thioamide-containing polymers are predominantly restricted to step-growth polycondensation strategies (two-component),[27,28] and more recently developed multicomponent polymerizations (Fig. 1a),[29–31] both of which limit architectural control and many of the advantages associated with chain-growth methods. Post-polymerization thionation (Fig. 1b) of pendant oxoamides using sulfurizing reagents such as P_4S_{10} or Lawesson's reagent have been explored,[15,16,32] but these reactions often suffer from incomplete conversion and generate problematic by-products that complicate purification.[33]

Thioimidates have been reported as a reversible protecting group for thioamides,[34] addressing the inherent fragility of thioamides during the synthesis of peptide biopolymers.[35–39] We recently provided the first demonstration of thioimidate compatibility with radical species and identified the structural features that enable radical-mediated polymerization of acrylate monomers bearing thioimidates in the side chain.[40] Here, we show that thioimidate-functionalized chain-growth polymers can be cleanly and efficiently converted into thioamides (Fig. 1c), producing only gaseous by-products to simplify purification. This strategy provides the first examples of thioamide-functional polymers accessed through radical polymerization.

Department of Chemistry, Iowa State University, Ames, IA 50011, USA.
E-mail: sdemirci@iastate.edu, bvv@iastate.edu

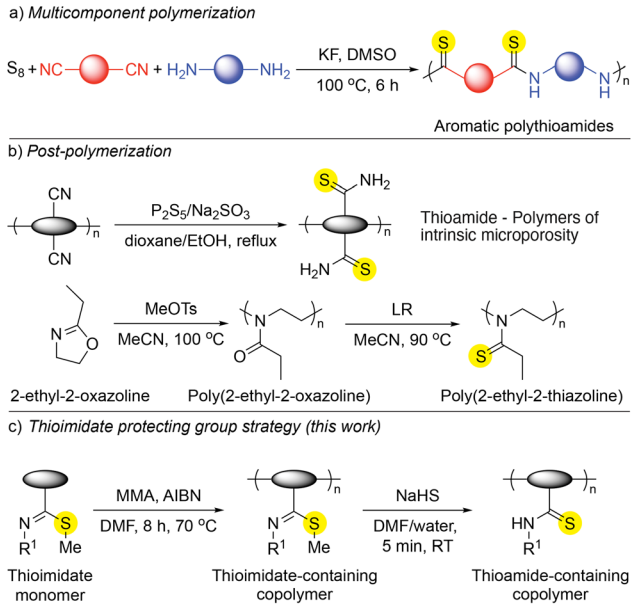

Fig. 1 Schematic representation of different synthetic strategies for thioamide containing polymers: (a) multicomponent polymerization, (b) post-polymerization, and (c) thioimidate protecting group strategy.

Table 1 Molecular characteristics and compositions of the poly(MMA-*co*-TIM) precursor copolymers and the corresponding thioamide-containing poly(MMA-*co*-TA) products obtained after NaHS-mediated post-polymerization modification

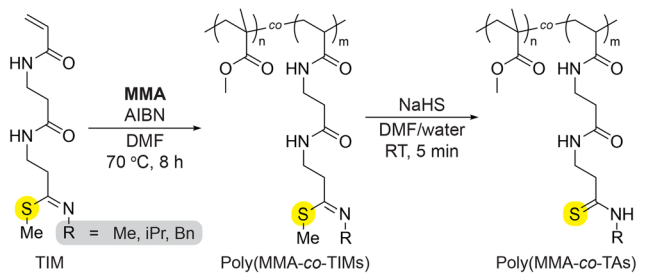

Thioimidate copolymers	$M_{n,SEC}$ (kg mol^{-1})[40]	Conv.[c] (%)	Incorporated TIM (mol%)[40]	Incorporated TA[d] (mol%)
MeTIM	14.0[a]	72.6	3.7	3.7
	24.3[b]	63.7	2.2	2.2
iPrTIM	15.4[a]	70.7	16.7	12.5
	22.2[b]	60.4	5.9	5.6
BnTIM	11.2[a]	55.2	12.5	12.5
	27.1[b]	66.5	4.8	4.8

$M_{n,SEC}$ values were determined by SEC using PMMA standards. [a] Feed molar ratio of MMA : thioimidate : initiator was 50 : 50 : 1. [b] Feed molar ratio of MMA : thioimidate : initiator was 100 : 100 : 1. [c] Monomer conversion determined gravimetrically. [d] Incorporated TA contents were determined by ^{1}H NMR.

Results and discussion

Given the importance of monomer accessibility, the thioimidate monomers MeTIM, iPrTIM, and BnTIM were prepared according to our recently reported multigram-scale protocol, which provides stable monomers suitable for free-radical polymerization.[40] Initial homopolymerization experiments with the thioimidate monomers gave only low molecular weight material at low conversion. Consequently, we targeted copolymerization with MMA to incorporate thioimidate units into chain growth polymers. Three thioimidate-containing copolymers were synthesized *via* free radical polymerization of thioimidate monomers (MeTIM, iPrTIM, and BnTIM) with methyl methacrylate (MMA) using AIBN as the initiator in DMF at 70 °C for 18 hours. The resulting poly(MMA-*co*-TIMs) copolymers were isolated and characterized by size-exclusion chromatography (SEC) to determine molecular weight and dispersity.[40] Table summarizes the molecular characteristics of all synthesized copolymers, with number-average molecular weights (M_n) ranging from 11.2 to 15.4 kg mol^{-1} and thioimidate incorporations of 3.7 to 16.7 mol% as determined by nuclear magnetic resonance spectroscopy. The dispersity values ($Đ$ = 1.2–1.4) reflect the precipitation and redispersion of the copolymers in cold diethyl ether prior to SEC analysis, which selectively removes low-molecular-weight oligomeric fractions and narrows the observed distribution. These values confirm that the thioimidate-functionalized monomers are compatible with radical chain-growth polymerization. Although the monomers were introduced at an equimolar MMA : TIM feed ratio, the resulting copolymer contained a greater fraction of MMA (Table 1). This deviation is attributable to steric constraints imposed by the bulky TIM side chains,[40–43] as well as inherent differences in polymerization reactivity between acrylate and acrylamide monomers.[44,45]

The poly(MMA-*co*-TIMs) were converted to thioamide-containing copolymers (poly(MMA-*co*-TAs)) using sodium hydrosulfide (NaHS) in a DMF/water mixture at room temperature for 5 minutes (Table 1). The conversion was efficiently achieved under these mild conditions, with gaseous by-products that simplify purification compared to traditional post-polymerization thionation methods. A practical limitation of this protocol is the formation of methyl mercaptan (methanethiol, CH_3SH) as a volatile by-product, which, due to its strong odor and toxicity, necessitates operation in a well-ventilated fume hood and would require appropriate gas-handling measures for larger-scale implementations.

The thioimidate-to-thioamide conversion was clearly observable and quantifiable in the ^{1}H NMR spectra (Fig. S2–S4). Upon NaHS treatment, the diagnostic thioimidate S–Me singlet at 2.46 ppm disappeared completely, confirming full consumption of the thioimidate functionality. Consistent with this clean conversion, the characteristic resonances of the comonomer units were retained at 3.50 ppm for the poly(MMA-*co*-MeTA) N–CH_3 group, 4.10 and 1.48 ppm for the poly(MMA-*co*-iPrTA) methine (–CH–) and methyl (–CH_3) groups, respectively, 4.80 ppm for the poly(MMA-*co*-BnTA) benzylic –CH_2– group, and 3.62 ppm for the MMA backbone –CH_3 group. The integrals of these TA-derived signals relative to the MMA –CH_3 resonance remained essentially unchanged before and after NaHS

treatment, indicating that the relative incorporation of TA comonomers and MMA units, as well as the backbone-to-pendant-unit ratios, are preserved during modification.

In the FTIR spectra of the poly(MMA-*co*-TAs), a characteristic band at 1436 cm^{-1} is observed, consistent with the C=S stretching vibration of thioamide groups. Comprehensive ^1H NMR and FTIR characterizaton – full spectra, stacked comparisons of thioimidate and thioamide copolymers, and peak assignments for all copolymers – is provided in the SI. Size-exclusion chromatography (SEC) traces are also shown in Fig. S8 for all poly(MMA-*co*-TIM) samples before NaHS treatment and for a representative poly(MMA-*co*-BnTA) sample after post-polymerization modification. For this representative example, SEC reveals no significant change in number-average molecular weight or dispersity upon NaHS treatment ($Đ$ = 1.3, compared to $Đ$ = 1.4 for the poly(MMA-*co*-BnTIM) precursor). Together with the preserved MMA/thioimidate and MMA/thioamide integration ratios in the ^1H NMR spectra, this indicates that the NaHS-mediated transformation proceeds with high conversion and without detectable main-chain degradation, coupling, or aggregation, and primarily converts the pendant thioimidate groups to thioamides.

Further confirmation of thioamide incorporation into the copolymer was obtained by examining its metal-binding properties, specifically its ability to extract metal ions from aqueous solution. After NaHS treatment, the poly(MMA-*co*-TAs) samples were thoroughly washed, and this washing procedure was repeated until methylene blue analysis confirmed the absence of free sulfide in the final wash fractions. Preliminary metal-ion selectivity experiments with Cu^{2+}, Fe^{3+}, Au^{3+}, and Pt^{4+} showed that the thioamide-containing copolymers preferentially extract Au^{3+} and Pt^{4+} while exhibiting negligible uptake of Cu^{2+} and Fe^{3+} under identical batch conditions, consistent with selective binding of noble-metal ions by the installed thioamide groups (Fig. 2). After establishing this selectivity profile, we investigated Au^{3+} adsorption in greater detail because gold recovery was used here as the proof-of-concept application for these thioamide-functional polymers. Varying amounts of the solid poly(MMA-*co*-TIMs) and poly(MMA-*co*-TAs) samples were then dispersed in the Au^{3+} solutions and stirred for 2 hours at room temperature. The insoluble polymeric adsorbents were separated by centrifugation and the remaining Au^{3+} concentrations were quantified by UV-Vis spectroscopy to determine extraction efficiency, which was defined as the mass of Au^{3+} removed divided by the mass of adsorbent added.

The thioamide-containing copolymers (poly(MMA-*co*-TAs)) exhibited gold adsorption capacities: poly(MMA-*co*-MeTA) = 51.4 mg g^{-1}, poly(MMA-*co*-iPrTA) = 42.6 mg g^{-1}, and poly(MMA-*co*-BnTA) = 38.9 mg g^{-1} (Fig. 3a), consistent with the introduction of metal-binding thioamide groups within the polymers. In sharp contrast, the thioimidate precursor poly(MMA-*co*-TIM) copolymers showed negligible Au^{3+} extraction efficiency, providing a compelling experimental confirmation of the conversion of thioimidate into thioamide.

The methyl-substituted variant poly(MMA-*co*-MeTA) demonstrated markedly superior adsorption capacity compared to the isopropyl and benzyl analogs, a difference attributed to the enhanced reactivity and accessibility of the methyl-bearing thioamide coordination sites. Furthermore, poly(MMA-*co*-

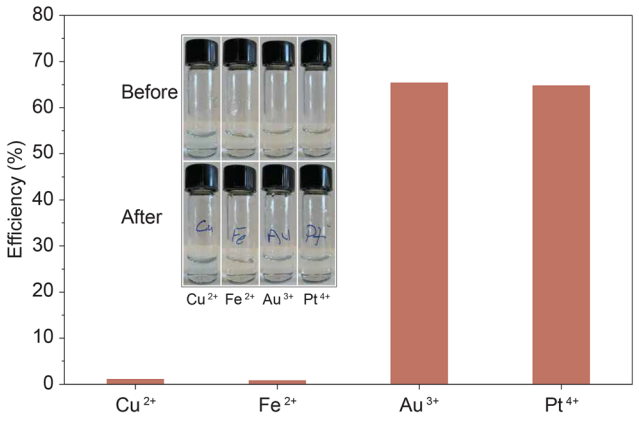

Fig. 2 Metal-ion selectivity of the thioamide-containing polymer under batch adsorption conditions. Photographs of metal-ion solutions (Cu^{2+}, Fe^{3+}, Au^{3+}, and Pt^{4+}) before and after treatment with the poly(MMA-*co*-BnTA).

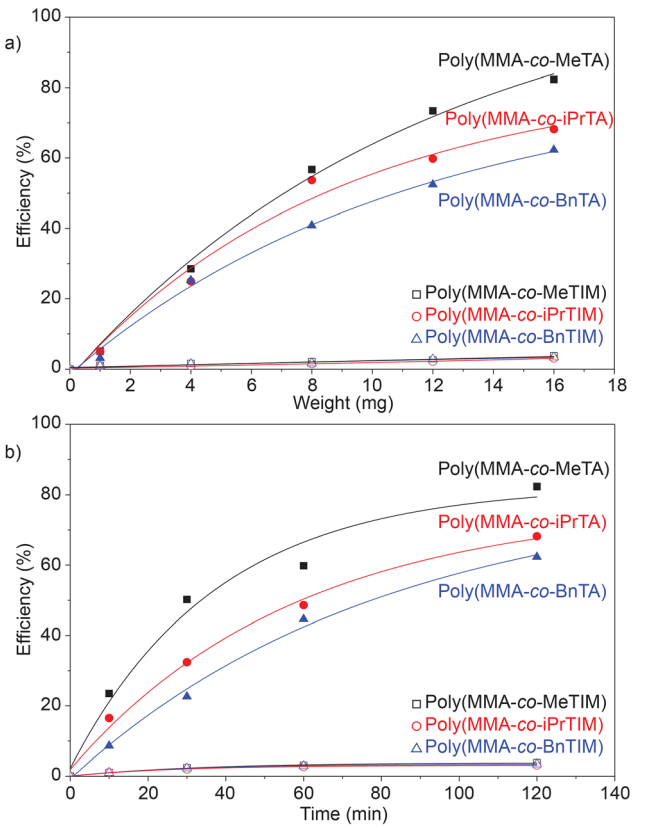

Fig. 3 Effect of adsorbent dosage (a) and contact time (b) on Au^{3+} extraction by poly(MMA-*co*-TIMs) (feed ratio MMA : TIM : initiator = 50 : 50 : 1) and poly(MMA-*co*-TAs) with comparable thioamide incorporations (Table 1). Data reported per mass of polymer to account for slight compositional differences and reflect thioamide site density effects.

MeTA) achieved more rapid Au^{3+} extraction with the initial rate of adsorption approximately twice as fast as those observed for poly(MMA-*co*-iPrTA) and poly(MMA-*co*-BnTA) (Fig. 3b). These findings underscore the critical role of the R-substituent in modulating both the affinity and kinetics of Au^{3+} coordination to the thioamide sulfur and nitrogen centers. Poly(MMA-*co*-MeTA), poly(MMA-*co*-iPrTA), and poly(MMA-*co*-BnTA) have similar but not identical thioamide incorporations, as summarized in Table 1. To avoid confounding effects from changes in solution viscosity and mass transfer, all Au^{3+} adsorption experiments in Fig. 3 were performed at a constant polymer mass loading rather than adjusting the total polymer concentration to equalize thioamide content. Consequently, the capacities in Fig. 3 are reported on a mass-of-polymer basis and reflect the combined influence of thioamide site density and the intrinsic binding characteristics of the different *N*-substituents; under these constant-mass conditions, the Me-substituted thioamide copolymer (MeTA) consistently exhibits higher Au^{3+} uptake than the iPr- and Bn-substituted analogues.

To extend the synthetic strategy toward more robust materials suitable for practical applications, thioimidate-containing cross-linked polymers (TIM-CLP) were prepared *via* free radical polymerization of thioimidate monomers (BnTIM) with ethylene glycol dimethacrylate (EGDMA) as a cross-linker (Fig. 4a). The resulting cross-linked polymers were chemically transformed to thioamide-functionalized materials (TA-CLP) under the same mild conditions employed for the linear copo-

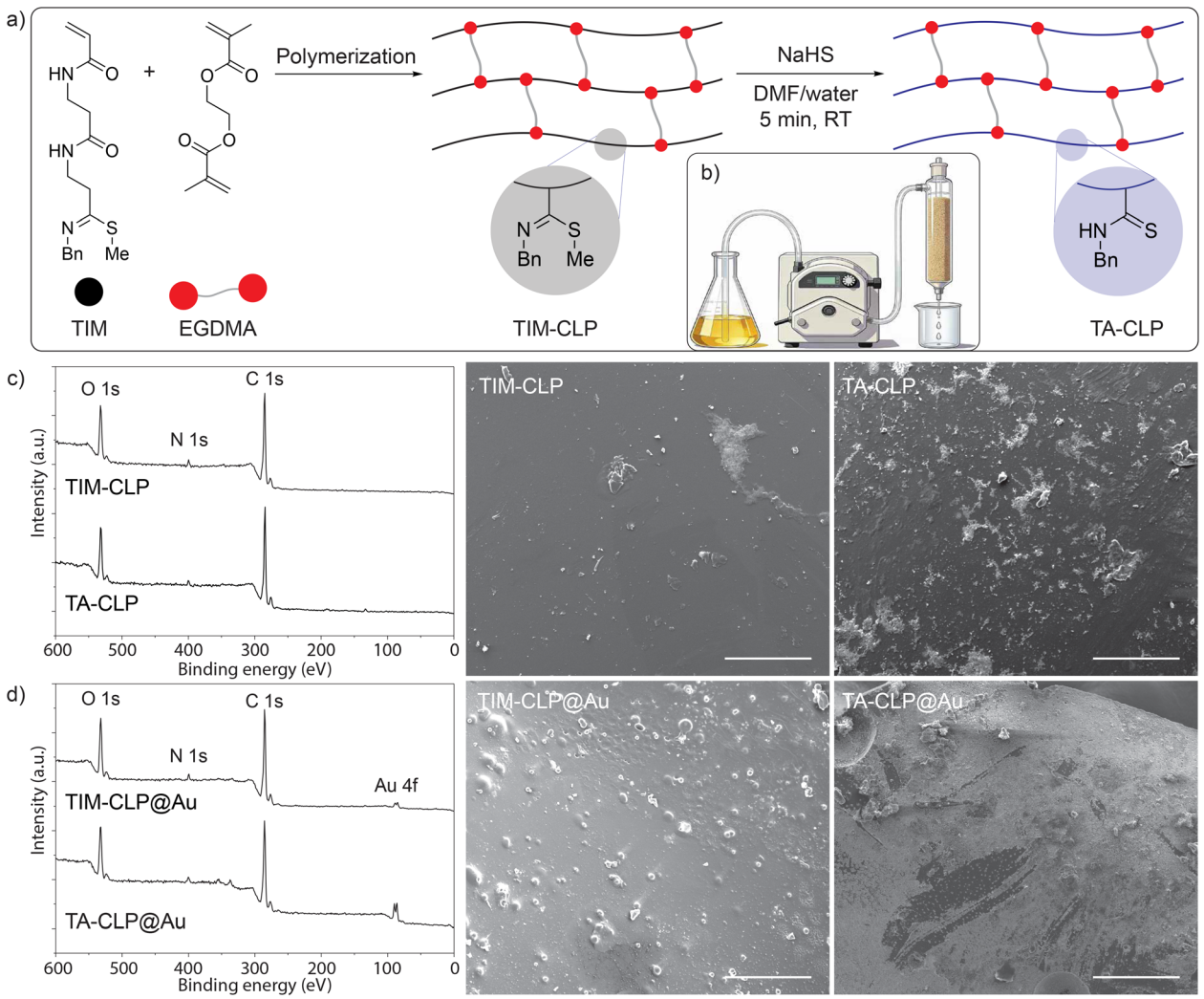

Fig. 4 Synthesis, characterization, and application of cross-linked polymer adsorbents for gold recovery. (a) Schematic illustration of the preparation of TI-CLP polymer *via* free radical polymerization of TIM with EGDMA cross-linker, followed by chemical modification to introduce thioamide functional groups. Subsequent deprotection yields the corresponding TA-CLP adsorbent material. (b) Schematic diagram of fixed bed column used in adsorption study of Au^{3+} onto adsorbent material. (c) XPS spectra and SEM images of pristine TIM-CLP and TA-CLP adsorbents, demonstrating surface chemical composition and particle morphology prior to adsorption. (d) XPS spectra and SEM micrographs of TIM and TA adsorbents after gold adsorption experiments, confirming successful gold uptake and surface modification. XPS binding energies and SEM magnifications are indicated where applicable. The scale bar is 100 μm.

lymers. In addition, after NaHS treatment the TA-CLP adsorbents were subjected to the same methylene blue assay used for the linear polymers, and repeated washing was performed until no free sulfide was detectable in the final wash fractions. The complete transformation of thioimidate to thioamide was corroborated by detailed elemental analysis by XPS (Table S1), confirming that the chemical conversion strategy was equally effective for cross-linked architectures.

To assess their viability as practical adsorbents, the TA-CLP material was subsequently evaluated as a packed-bed column adsorbent for continuous gold recovery applications (Fig. 4b). The fixed-bed column setup consisted of a feed reservoir containing the Au^{3+} solution, a peristaltic pump for controlled flow delivery, and a column packed with TIM-CLP and TA-CLP adsorbent materials, enabling systematic evaluation under dynamic flow conditions.

Both XPS and SEM were employed to document the material properties before (Fig. 4c) and after (Fig. 4d) Au^{3+} adsorption. XPS measurements of both materials after exposure to Au^{3+} revealed negligible Au signal for TIM-CLP, but a 5-fold increase in Au 4f photoelectron signals (binding energies of 84.0 eV for Au $4f_{7/2}$ and 87.7 eV for Au $4f_{5/2}$) for TA-CLP. The morphological results from SEM confirm these findings. Notably, TA-CLP@Au surfaces displayed visible particulate accumulation and increased roughness from surface-bound gold, indicating thioamide coordination sites with substantially higher gold adsorption capacity.

Fixed-bed column tests identified the TA-CLP as a robust Au^{3+} adsorbent, motivating equilibrium characterization by batch Langmuir isotherm analysis (Fig. 5). TA-CLP exhibited a maximum Au^{3+} adsorption capacity of 38.17 mg g^{-1} and a Langmuir affinity constant K_m = 5.45 × 10^{-2} mL μg^{-1}; with an excellent linear fit (R^2 = 0.9877) to the Langmuir model, consistent with monolayer adsorption on a relatively homogeneous population of binding sites, as typically assumed for Langmuir-type systems. The corresponding dimensionless separation factors (R_L), calculated over the investigated concentration range, all fall between 0 and 1 (Table S2), indicating that Au^{3+} uptake on TA-CLP proceeds under thermodynamically favorable conditions according to the conventional Langmuir criteria.[46,47] Although these capacities are lower than those of highly engineered S/N-rich adsorbents that can reach several hundred mg g^{-1} for Au^{3+},[48–50] they compare well with simpler functionalized polysaccharides and polymer gels, which typically exhibit Au^{3+} capacities below ~mg g^{-1}.[51,52] In combination with the linear thioamide copolymers (q_m up to 51.4 mg g^{-1}), these results demonstrate that thioamide-functionalized chain-growth polymers provide practically relevant Au^{3+} uptake while offering a modular postpolymerization platform to tune binding site density and polymer architecture for precious metal recovery. Efforts to increase the ratio of thioimidate monomer incorporation in to the polymers is currently underway to improve the metal-absorbing capacity.

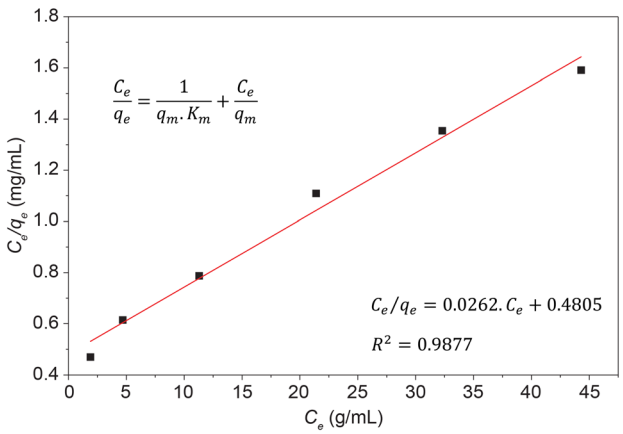

Fig. 5 Adsorption isotherms of Au^{3+} on TA-CLP, linearized according to the Langmuir equation.

Conclusion

This work demonstrates that the thioimidate protecting-group strategy enables the incorporation of thioamide functionalities into both linear and cross-linked radical chain-growth polymer architectures. Preliminary metal-ion selectivity experiments show that the resulting thioamide-containing materials preferentially bind noble-metal ions over base-metal ions, highlighting their potential for targeted metal separation. The linear copolymers exhibited Au^{3+} extraction capacities up to 51.4 mg g^{-1}, with the methyl-substituted variant displaying enhanced adsorption kinetics. The cross-linked platform afforded a robust three-dimensional adsorbent with a maximum adsorption capacity of 38.17 mg g^{-1} and favorable thermodynamic characteristics. Together, these findings expand the synthetic utility of thioimidates[34–38,53,54] as enabling functional handles for thioamide installation in chain-growth polymers and validate the strong and selective coordination of noble-metal ions by the resulting materials for precious metal recovery.

Experimental

All experimental details and characterization data are provided in the SI.

Author contributions

All authors conceptualized the work and designed experiments. S. K. D. synthesized monomers. S. D. carried out polymerization and gold-binding experiments. S. D. and B. V. wrote the manuscript.

Conflicts of interest

No conflicts to declare.

Data availability

All experimental details and characterization data are provided in the supplementary information (SI) and available free of charge on the publisher's website for this article.

Supplementary information: experimental details, NMR and FTIR spectra, and SEC traces. See DOI: https://doi.org/10.1039/d6py00344c.

Acknowledgements

The authors acknowledge the National Science Foundation under award number 2404390. We thank Dr Sarah Cady and Dr Kamel Harrata of the Iowa State University Chemical Instrumentation Facility for training and support related to the NMR and MS measurements reported in this work. SEM and XPS analyzes were performed at the Materials Analysis and Research Laboratory, Iowa State University, and we thank Dr Warren Straszheim for SEM and Dr Dapeng Jing for XPS characterization.

References

1 T. N. Hansen and C. A. Olsen, *Chem. – Eur. J.*, 2024, **30**, e202303770.
2 G. Huang, T. Cierpicki and J. Grembecka, *Eur. J. Med. Chem.*, 2024, **277**, 116732.
3 N. Mahanta, M. Szantai-Kis, E. J. Petersson and D. A. Mitchell, *ACS Chem. Biol.*, 2019, **14**, 142.
4 B. J. Lampkin and B. VanVeller, *J. Org. Chem.*, 2021, **86**, 18287–18291.
5 C. R. Walters, D. M. Szantai-Kis, Y. Zhang, Z. E. Reinert, W. S. Horne, D. M. Chenoweth and E. J. Petersson, *Chem. Sci.*, 2017, **8**, 2868–2877.
6 R. W. Newberry, B. VanVeller and R. T. Raines, *Chem. Commun.*, 2015, **51**, 9624–9627.
7 K. E. Fiore, M. J. Patist, S. Giannakoulias, C.-H. Huang, H. Verma, B. Khatri, R. P. Cheng, J. Chatterjee and E. J. Petersson, *RSC Chem. Biol.*, 2022, **3**, 582–591.
8 H. Verma, B. Khatri, S. Chakraborti and J. Chatterjee, *Chem. Sci.*, 2018, **9**, 2443–2451.
9 P. Ghosh, N. Raj, H. Verma, M. Patel, S. Chakraborti, B. Khatri, C. M. Doreswamy, S. Anandakumar, S. Seekallu, M. Dinesh, *et al.*, *Nat. Commun.*, 2023, **14**, 6050.
10 T. M. Barrett, X. S. Chen, C. Liu, S. Giannakoulias, H. A. T. Phan, J. Wang, E. K. Keenan, R. J. J. Karpowicz and E. J. Petersson, *ACS Chem. Biol.*, 2020, **15**, 774–779.
11 H. A. T. Phan, Y. Chang, S. A. Eaton and E. J. Petersson, *Chem. Commun.*, 2024, **60**, 13075–13078.
12 N. Mahanta, D. M. Szantai-Kis, E. J. Petersson and D. A. Mitchell, *ACS Chem. Biol.*, 2019, **14**, 142–163.
13 R. W. Newberry, B. VanVeller, I. A. Guzei and R. T. Raines, *J. Am. Chem. Soc.*, 2013, **135**, 7843–7846.
14 Y. Huang, R. Hu and B. Z. Tang, *Macromolecules*, 2024, **57**, 6568–6576.
15 A. Mathianaki, A. K. Demeler, A. Dömling, F. Ferrari, F. C. M. Scheelje, H. Bahmann and G. Delaittre, *Polym. Chem.*, 2025, **16**, 301–307.
16 A. Hacioglu, V. Baddam, A. Kerr, J. Kehrein, A. Bunker and R. Luxenhofer, *Macromolecules*, 2024, **57**, 10368–10378.
17 K. Bayram, B. Kiskan and Y. Yagci, *Polym. Chem.*, 2021, **12**, 534–544.
18 M. Sharma, C. Patel, S. Sriram, S. Mukherjee and A. K. Das, *ACS Appl. Polym. Mater.*, 2023, **5**, 10065–10072.
19 S. Kagaya, H. Miyazaki, M. Ito, K. Tohda and T. Kanbara, *J. Hazard. Mater.*, 2010, **175**, 1113–1115.
20 H. Xiang, J. Wang, Z. Guo, Y. Chen, B. Jiang, S. Ye and W. Yi, *Angew. Chem.*, 2023, **135**, e202313779.
21 X. Li, C. Zhang, R. Zhao, X. Lu, X. Xu, X. Jia, C. Wang and L. Li, *Chem. Eng. J.*, 2013, **229**, 420–428.
22 H. Zhou, W. Zhao, S. Zhang, X. An, H. Lan, H. Liu and J. Qu, *Resour., Conserv. Recycl.*, 2023, **198**, 107165.
23 W. Cao, F. Dai, R. Hu and B. Z. Tang, *J. Am. Chem. Soc.*, 2019, **142**, 978–986.
24 L. Huang and Q. Shuai, *ACS Sustainable Chem. Eng.*, 2019, **7**, 9957–9965.
25 H. Watanabe and M. Kamigaito, *J. Am. Chem. Soc.*, 2023, **145**, 10948–10953.
26 B. Lepoittevin, J. Baudoux, D. Bray, A. Gonzalo-Barquero and J. Rouden, *React. Funct. Polym.*, 2023, **192**, 105731.
27 Y. Kishimoto and N. Ogata, *Polym. J.*, 1973, **4**, 637–643.
28 I. Delfanne and G. Levesque, *Macromolecules*, 1989, **22**, 2589–2592.
29 W. Li, X. Wu, Z. Zhao, A. Qin, R. Hu and B. Z. Tang, *Macromolecules*, 2015, **48**, 7747–7754.
30 T. Kanbara, Y. Kawai, K. Hasegawa, H. Morita and T. Yamamoto, *J. Polym. Sci., Part A: Polym. Chem.*, 2001, **39**, 3739–3750.
31 F. Z. Ramdane, G. Tabak, K. Nassima and A. Benaboura, *Polym. Sci., Ser. B*, 2017, **59**, 443–451.
32 C. R. Mason, L. Maynard-Atem, N. M. Al-Harbi, P. M. Budd, P. Bernardo, F. Bazzarelli, G. Clarizia and J. C. Jansen, *Macromolecules*, 2011, **44**, 6471–6479.
33 G. Tabak, T.-N. Pham, G. Levesque and R. Haraoubia, *J. Polym. Sci., Part A: Polym. Chem.*, 1998, **36**, 117–127.
34 J. Byerly-Duke, E. A. O'Brien, B. J. Wall and B. VanVeller, *Methods in enzymology*, Elsevier, 2024, vol. 698, pp. 27–55.
35 L. A. Camacho III, B. J. Lampkin and B. VanVeller, *Org. Lett.*, 2019, **21**, 7015–7018.
36 L. A. Camacho III, Y. H. Nguyen, J. Turner and B. VanVeller, *J. Org. Chem.*, 2019, **84**, 15309–15314.
37 J. Byerly-Duke and B. VanVeller, *Org. Lett.*, 2024, **26**, 1452–1457.
38 J. Byerly-Duke, A. Donovan, E. A. O'Brien, K. K. Sharma, R. Ibrahim, L. M. Stanley and B. VanVeller, *J. Org. Chem.*, 2024, **89**, 14755–14761.
39 B. J. Wall, U. Chaudhury, K. K. Sharma and B. VanVeller, *J. Am. Chem. Soc.*, 2026, **148**, 16482–16492.

40 S. Kinali-Demirci, S. Demirci, J. Byerly-Duke and B. VanVeller, *Angew. Chem., Int. Ed.*, 2025, e202509727.
41 X. Wang and N. Hadjichristidis, *Angew. Chem.*, 2021, **133**, 22643–22651.
42 H. S. Bisht, S. S. Ray and A. K. Chatterjee, *J. Polym. Sci., Part A: Polym. Chem.*, 2003, **41**, 1864–1866.
43 P. Maksym, M. Tarnacka, A. Dzienia, K. Wolnica, M. Dulski, K. Erfurt, A. Chrobok, A. ZiÈ©ba, A. Brzózka, G. Sulka, *et al.*, *RSC Adv.*, 2019, **9**, 6396–6408.
44 D. Neugebauer and K. Matyjaszewski, *Macromolecules*, 2003, **36**, 2598–2603.
45 U. C. Palmiero, A. Chovancová, D. Cuccato, G. Storti, I. Lacík and D. Moscatelli, *Polymer*, 2016, **98**, 156–164.
46 S. Demirci and T. Caykara, *Mater. Sci. Eng., C*, 2013, **33**, 111–120.
47 S. Demirci, A. Celebioglu and T. Uyar, *Carbohydr. Polym.*, 2014, **113**, 200–207.
48 R. Ding, Y. Chen, Y. Li, Y. Zhu, C. Song and X. Zhang, *ACS Appl. Mater. Interfaces*, 2022, **14**, 11803–11812.
49 S. Abubakar, G. Das, T. Prakasam, A. Jrad, F. Gándara, S. Varghese, T. Delclos, M. A. Olson and A. Trabolsi, *ACS Appl. Mater. Interfaces*, 2024, **17**, 17794–17803.
50 Y. Wu, D. Xiang, M. Zhu, Y. Chen, J. Luo and S. Wang, *J. Phys. Chem. B*, 2025, **129**, 10131–10145.
51 Y. Fan, Q. Zhou, S. Zhang and Y. Nie, *Int. J. Biol. Macromol.*, 2024, **274**, 133481.
52 I. Dakova, O. Veleva and I. Karadjova, *Molecules*, 2024, **29**, 4970.
53 B. J. Wall, K. K. Sharma, E. A. O'Brien, A. Donovan and B. VanVeller, *J. Am. Chem. Soc.*, 2024, **146**, 11648–11656.
54 E. A. O'Brien, K. K. Sharma, J. Byerly-Duke, L. A. Camacho III and B. VanVeller, *J. Am. Chem. Soc.*, 2022, **144**, 22397–22402.